analytical chemistry

pubs.acs.org/ac Article

A Multitargeted Electrochemiluminescent Biosensor Coupling DNAzyme with Cascading Amplification for Analyzing Myocardial miRNAs

Yudie Sun,[‖] La Fang,[‖] Zhe Zhang, Yang Yi, Shengjun Liu, Qian Chen, Jian Zhang, Cheng Zhang, Lifang He, and Kui Zhang*

Cite This: *Anal. Chem.* 2021, 93, 7516−7522 Read Online

ACCESS | Metrics & More | Article Recommendations | Supporting Information

ABSTRACT: Several circulating miRNAs are associated with the pathogenic process of acute myocardial infarction (AMI). Thus, analyzing myocardial miRNAs in the circulatory system is important for the diagnosis and treatment of AMI, especially for early-stage diagnosis. Based on the characteristics of myocardial miRNAs, an ultrasensitive and multitargeted electrochemiluminescence (ECL) sensing platform was developed with a versatile probe that can couple DNAzyme with hybridization chain reaction amplification. The target miRNA and auxiliary chains form a circular unit that shears the versatile probe hairpin, and the products subsequently trigger cascading amplification; a long strand of dsDNA is then generated with many C-rich sequences that can undergo in situ reductions to generate ECL luminophore silver clusters. Using this strategy, three myocardial miRNAs are successfully detected with a detection limit as low as 29.6 aM (S/N = 3). Notably, our method can detect myocardial miRNA groups composed of multiple related circulating miRNAs with high selectivity over interfering miRNAs in blood. This is extremely important for solving the problem of diverse and low abundance of infarct-associated miRNAs. Our strategy pioneers a new idea of miRNA detection, and given its versatility and sensitivity, it is promising for the diagnosis of multigene-regulated cardiovascular diseases.

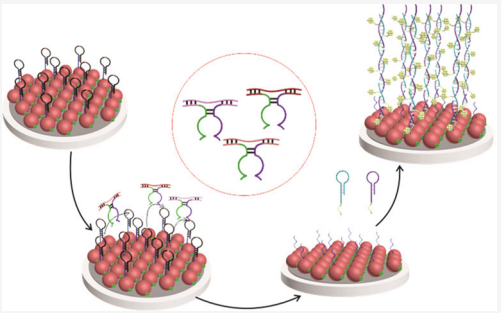

INTRODUCTION

Acute myocardial infarction (AMI) is a cardiovascular lesion that can bring the heart to a rapid halt and result in high mortality rates.[1−4] Multiple biologically active substances are present in blood at the onset of AMI, and some markers change with the stage of AMI progression. Current studies have confirmed the presence of AMI-related miRNAs in the circulatory system.[5−7] These miRNAs can exist stably in blood, and the type and expression of miRNAs vary greatly along different pathological stages. Therefore, miRNAs in blood are ideal biomarkers for the diagnosis or prognosis of infarct disease.[8] Considering the characteristics of AMI and the complexity of the blood environment, the establishment of stable, efficient, and precise analytical methods for myocardial miRNAs is currently a hot topic in AMI early diagnosis.[9] It is important to develop sensitive detection methods for the analysis of multiple myocardial miRNAs and relevant miRNA groups.[10−12]

Recently, by combining novel sensing principles with advanced spectral techniques, researchers have made much progress in the analysis of miRNAs in myocardial infarction.[13−16] Initially, as chemiluminescence (CL) was considered the most promising for point-of-care detection, researchers combined new CL materials with highly efficient amplification techniques to build multiple biosensors for miRNA detection with mobile phones.[17−19] However, CL was not suitable for simultaneous detection of multiple miRNAs. Subsequently, researchers made use of the high-throughput detection of surface-enhanced Raman spectroscopy (SERS) and established a biological affinity probe-facilitated SERS sensing platform for myocardial miRNA.[20] However, SERS has some inherent bottlenecks in biosensors that need to be further addressed. Soon afterward, ECL attracted great interest in myocardial miRNA analysis, and several ECL sensors were developed, improving detection sensitivity.[21−24] ECL was more suitable for miRNA detection of myocardial infarction due to its simple equipment, high sensitivity and repeatability, and controllable potential.

Catalytic nucleic acid DNAzyme has attracted more and more attention as the amplification component of sensors.[25−27] Similar to proteases, DNAzyme has high selectivity and strong catalytic activity. In addition, DNAzyme has the advantages of

Received: March 9, 2021
Accepted: April 26, 2021
Published: May 4, 2021

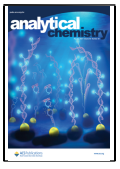

https://doi.org/10.1021/acs.analchem.1c01051
Anal. Chem. 2021, 93, 7516−7522

Scheme 1. Schematic Illustration of the Multitargeted ECL Biosensor for Analyzing Myocardial miRNAs

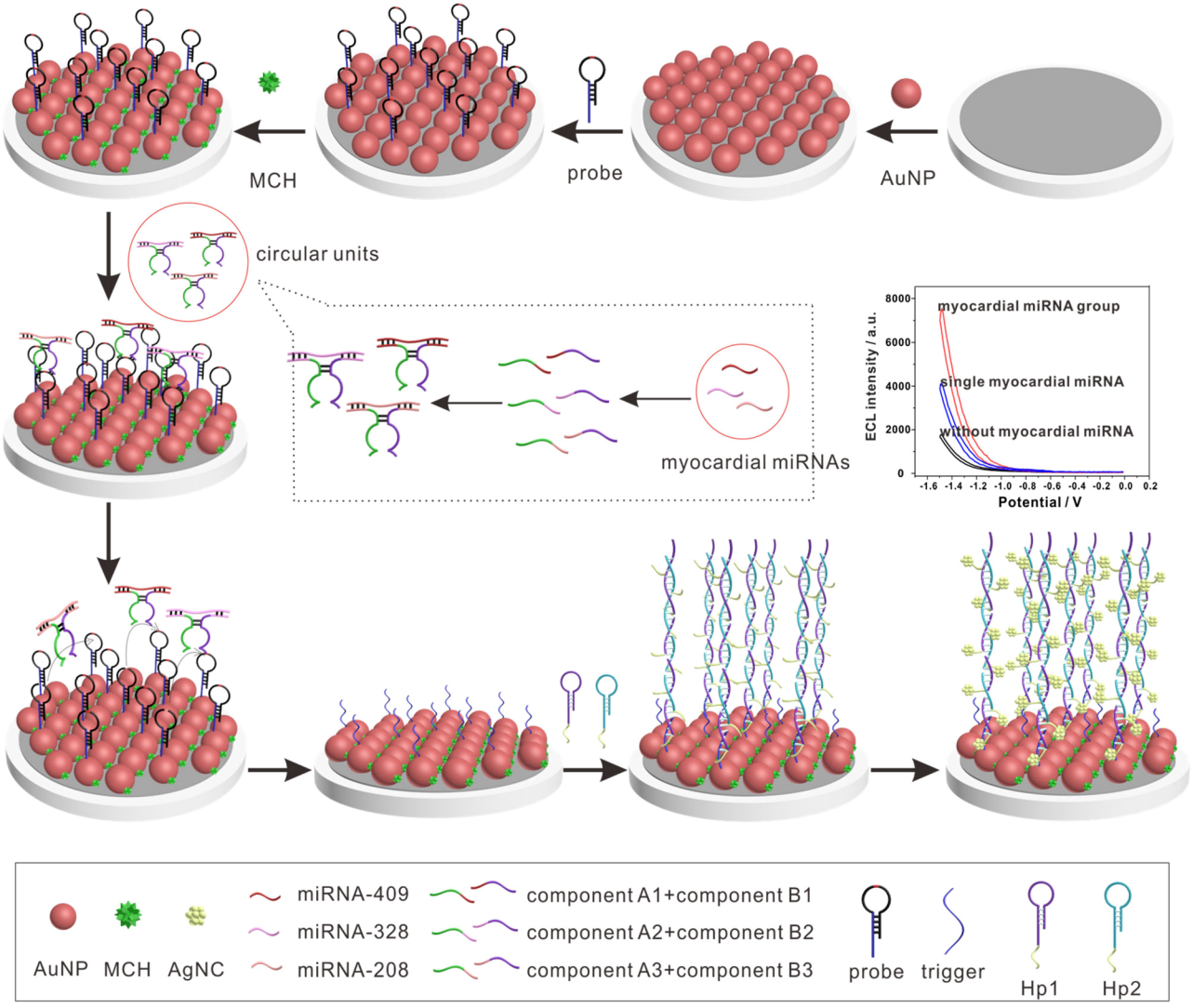

easy synthesis, easy modification, good stability, and low production cost compared with proteases. DNAzyme is often used as a biosensitive element for improving sensing performance in biological analysis platforms.[28−30] The assembly scheme of active DNAzyme opens up a new method of miRNA analysis in myocardial infarction.[18] By properly splitting DNAzyme and reasonably designing miRNA cycle structure, accurate identification and multiple cycle amplification of the target can be achieved. The combination of DNAzyme amplification with other amplification techniques to perform multilevel signal amplification improves the sensitivity of analysis under extreme conditions. Through further structural design and probe loading, this amplification scheme provides more insight into the ECL sensing platform of myocardial miRNA.

In this work, we designed a versatile probe for a multitargeted ECL biosensor based on a combination of active DNAzyme and hybridization chain amplification (HCR)[31] targeting myocardial miRNAs. As shown in Scheme 1, accurate capture of miRNA and sufficient signal amplification are achieved by a well-designed DNAzyme assembly with a target cyclic amplifying unit. Subsequently, the product on the versatile probe triggers HCR to generate dsDNA polymers with several C-rich sequences, which generates silver nanoclusters (AgNCs) by in situ reduction, thereby greatly enhancing the ECL signal. The combination of DNAzyme catalytic amplification and HCR induces AgNC ECL, which accurately identifies multiple miRNAs, effectively improving the sensitivity and repeatability of detection. With this method, multiple myocardial miRNAs and myocardial miRNA groups are detected with high sensitivity and selectivity.

EXPERIMENTAL SECTION

Materials and Reagents. We bought well-designed DNA from Sangon Biotechnology Company. Myocardial miRNAs chosen for detection were purchased from GemmaPharma Gene Company. The sequences of all mentioned genes in this work are listed in Table S1. RNase inhibitors, polyacrylamide, and tris were also ordered from Sangon Biotechnology Company. Chloroauric acid ($HAuCl_4$), silver nitrate ($AgNO_3$), trisodium citrate, sodium chloride (NaCl), 6-mercaptoethanol (MCH), potassium peroxydisulfate ($K_2S_2O_8$), and magnesium acetate ($MgAC_2$) were bought from Sinopharm Chemical Reagent Company. All ordered reagents were of analytical grade. The serum used in our work was provided by the Ma'anshan First People's Hospital.

https://doi.org/10.1021/acs.analchem.1c01051
Anal. Chem. 2021, 93, 7516−7522

Instrumentation. The ECL and EC measurements were performed on an MPI-type B multiparameter chemical analysis test system-electrochemical analyzer (Xi'an Reman Electronic Science & Technology Co., Ltd., Xi'an, China). The photomultiplier tube voltage was biased at 800 V. The potential scan was set from −1.6 to 0.2 V at a rate of 0.1 V·s^{-1}. The traditional three-electrode system was adopted in EC workstations, including a GCE (glassy carbon electrode) working electrode, a platinum wire counter electrode, and a reference electrode (Ag/AgCl). AgNCs were characterized using a transmission electron microscope (TEM) (JEM-2100). Nucleic acid electrophoresis results were captured using a Tanon-1600 gel imaging system. Ultrapure water (>18.2 MΩ) used in our experiment was purified using a Millipore purification system.

Polyacrylamide Gel Electrophoresis (PAGE). All gene sequences should be annealed at 90 °C for 10 min prior to nucleic acid reactions. Characterization of DNAzyme structure and digestion effects were taken after incubating in 10 mM TE buffer at 37 °C for 3 h. Since the composite structure is relatively complex, an excessive nucleic acid can cause channel congestion, so the concentration of a single nucleic acid chain was 0.1 μM and the total volume of each sample was 20 μL. PAGE electrophoresis (10%, w/w) for DNAzyme was performed in TA buffer at 96 V (10 h, 4 °C). However, a low product concentration is not enough to show the characteristics of HCR ladder bands, so the concentration of a single chain for characterization of HCR was 0.3 μM. After incubating, the results of HCR were analyzed by electrophoresis in TA buffer at 120 V for 2 h (6% PAGE, 25 °C).

Procedures for miRNA Recognition and Signal Amplification. The principle of recognition and amplification is displayed in Scheme 1. All the processes were performed on a AuNP-coated GCE. AuNPs with a diameter of about 18 nm were synthesized by a classical citrate synthesis method (as shown in Figure S1).[32] Then, the AuNP-coated electrodes were prepared according to the methods reported in the literature.[33] Briefly, AuNPs were coated by dropping a AuNP sol (10 μL) on the well-polished GCE surface and then dried naturally. For the DNAzyme composite structure, 10 μL of 1 M NaCl PB buffer containing a 3.0 μM versatile probe was first dropped onto the electrode for 4 h at 25 °C. Then, MCH is modified to the vacancy to prevent nonspecific binding. Finally, 1.0 μM auxiliary DNA strand component A and 1.0 μM auxiliary DNA strand component B were mixed with the corresponding target miRNA and incubated on the electrode for 3 h to form DNAzyme. For the subsequent cascade amplification process, the mixture of two hairpin DNAs was incubated with the DNAzyme product on the electrode at 37 °C for 3 h. A large number of C-rich sequences can be connected to the electrode surface in series through HCR to improve ECL signals.

Preparation of AgNCs for ECL Detection. Before the preparation of AgNCs, the electrode was washed to remove blood after the miRNA recognition and nucleic acid signal amplification process. Then, a modification of the synthetic method reported in the literature was made to synthesize AgNCs.[34,35] First, 8 μL of 100 μM $AgNO_3$ solution was transferred to the modified surface and reacted in the dark for 30 min. Then, 8 μL of 100 μM fresh $NaBH_4$ solution was dropped with the $AgNO_3$ solution and incubated in the dark at ambient temperature for 2 h. Finally, AgNCs were obtained for ECL measurement in 0.1 M PBS (pH 7.4), which contains 0.05 M $K_2S_2O_8$ and 0.1 M KCl.

RESULTS AND DISCUSSION

Design and Characterization of a Versatile Probe-Assisted Multitargeted ECL Biosensor for Myocardial miRNA Detection. We designed a versatile probe to combine DNAzyme amplification and HCR amplification for myocardial miRNA detection in an ECL biosensor. Multiple myocardial miRNAs were detected with high sensitivity using multistage amplification with high enzyme specificity. As shown in Scheme 1, the versatile probe was designed with RNA splice sites and sulfhydryl functional groups then modified on a AuNP-coated GCE. Before miRNA detection, the commonly used sealant MCH was filled into spaces on the electrode to prevent nonspecific adsorption.[13,36] In order to detect the target miRNA, two corresponding auxiliary DNA chains that form compound DNAzyme structures with the probe and target were added to the solution to be tested. Target myocardial miRNA and auxiliary strands (component A and component B) form circular structures, which form DNAzyme on the probe and continue cutting the rA sites. For multiple myocardial miRNA detection, all auxiliary strands corresponding to different target miRNAs were mixed and added to the sample. Although different targets form different circular units, they all form DNAzyme structures with the probe and cut the same rA site to form the same products. In this way, all expected myocardial miRNAs contribute to the ECL signal, thus making the myocardial miRNA group easier to be detected than a single miRNA, especially at very low levels in real samples. Subsequently, the residue chain of the versatile probe on the electrode was released to trigger HCR amplification, and a large number of C-rich AgNC template chains were anchored on the electrode. Finally, AgNCs were synthesized on a C-rich template by chemical reduction, and the successful synthesis of AgNCs is verified by electron microscopy (Figure S2).[35,37] This novel design employs not only the precise recognition capability of the enzyme but also the multistage amplification technology, endowing our ECL sensor with high sensitivity and accuracy in the analysis of myocardial miRNAs. By fine-tuning the sequence of auxiliary chains, the sensing platform can respond to different miRNAs and realize the detection of multiple miRNAs. In addition, by adding multiple auxiliary chains, the response to arbitrary miRNAs in myocardial miRNA groups can be achieved, which has great application prospects in clinical analysis.

To verify the feasibility of the design principle, the DNAzyme composite structure and the cascade amplification process were characterized by native PAGE (Figure 1). As shown in Figure 1A, when the gene under test is present, a new band is observed, indicating the formation of the circular unit (lane 4). When all the components are involved in the reaction, a new complete band appears, indicating the formation of the combined structure (lane 10). By comparing lane 10 and lane 11, only the DNAzyme structure formed by the probe with the rA site produces a new band, which happens to be in the same position as the expected product chain, proving that the digestion was conducted smoothly.

From Figure 1B, two stable hairpin DNA structures were formed for the HCR process (lanes 1 and 2). The DNAzyme-digested product unlocks the first hairpin DNA, indicated by the new band moving behind any hairpin DNA (lane 4). In the absence of DNAzyme-digested products, the two hairpin DNA

https://doi.org/10.1021/acs.analchem.1c01051
Anal. Chem. 2021, 93, 7516−7522

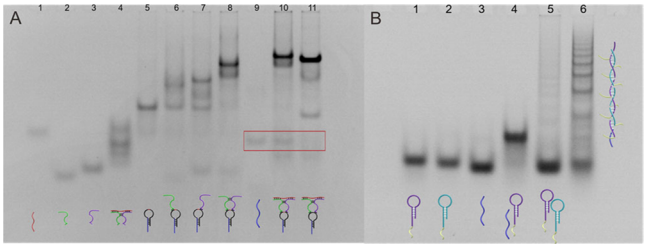

Figure 1. (A) 10% PAGE analysis of DNAzyme. Lane (1) target miRNA, (2) component A, (3) component B, (4) target miRNA + component A + component B, (5) versatile probe, (6) component A + versatile probe, (7) component B + versatile probe, (8) component A + component B + versatile probe, (9) DNAzyme-digested product, (10) target miRNA + component A + component B + versatile probe (with an rA site), (11) target miRNA + component A + component B + versatile probe (without an rA site). (B) 6% PAGE analysis of the HCR products. Lanes 1−6: hp1, hp2, DNAzyme-digested product, DNAzyme-digested product + hp1, hp1 + hp2, and DNAzyme-digested product + hp1 + hp2.

structures can coexist stably with low background noise (lane 5). Upon addition of DNAzyme-digested products, distinct HCR characteristic bands can be observed (lane 6).[38−40] The electrophoretogram shows that the DNAzyme digestion products can further trigger HCR amplification by elaborate design. The above gel electrophoresis results indicate that precise identification and multistage amplification are successfully coupled using a versatile probe.

Cyclic voltammograms (CVs) and electrochemical impedance spectroscopy (EIS) were carried out to analyze every step of the biosensor construction (shown in Figure 2A,B).

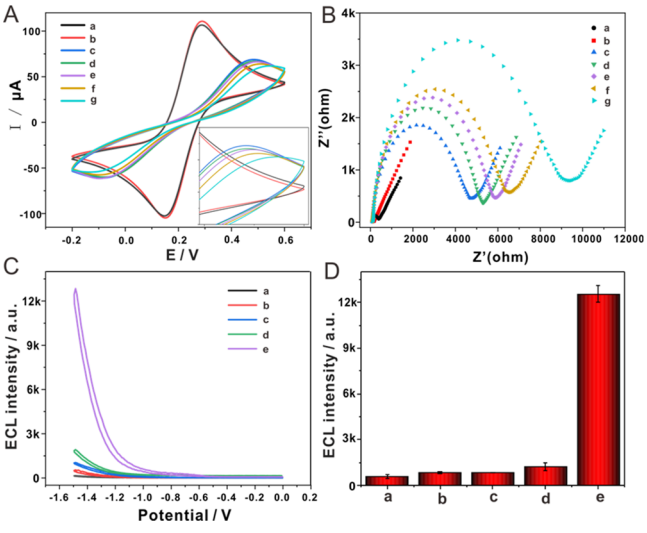

Figure 2. (A) CV and (B) EIS curves for characterizing the stepwise fabrication process of this ECL biosensor on electrodes: (a) GCE, (b) AuNP/GCE, (c) probe/AuNP/GCE, (d) MCH/probe/AuNP/GCE, (e) DNAzyme/MCH/probe/AuNP/GCE, (f) HCR/DNAzyme/MCH/probe/AuNP/GCE, and (g) AgNC/HCR/DNAzyme/MCH/probe/AuNP/GCE. The CV process was performed in 5.0 mM $[Fe(CN)_6]^{3-/4-}$ from −0.2 to 0.6 V with the scan rate of 0.1 V/s. (C) ECL potential curves and (D) ECL intensity of different modified electrodes for some important fabrication steps. (a) GCE, (b) MCH/probe/AuNP/GCE, (c) HCR/DNAzyme/MCH/probe/AuNP/GCE, (d) AgNC/HCR/DNAzyme/MCH/probe/AuNP/GCE without a target, and (e) AgNC/HCR/DNAzyme/MCH/probe/AuNP/GCE with a target.

The process begins with a finely polished GCE, which displays a definite redox peak of $[Fe(CN)_6]^{-3/-4}$ and a small EIS semicircle due to its thoroughly cleaned surface (curve a).[41,42] When AuNPs were assembled onto the GCE surface, the redox intensity rose slightly, and the semicircle was reduced to be negligible, indicating that the electrical conductivity was enhanced by AuNPs (curve b).[43,44] Subsequent modification of the versatile probe contributed to significant changes in CV and EIS measurements. As electron transfer was obstructed by the repulsive force of negatively charged DNA on $[Fe(CN)_6]^{-3/-4}$, the resistance (Ret) greatly increased, and the CV current significantly decreased (curve c).[45] After filling the remaining space on the electrode with MCH, the impedance further increased, and the current continued to decrease (curve d).[46] Afterward, DNAzymes were constructed with the versatile probes, and the augmented steric hindrance of the large nucleic acid-braided frame led to the semicircle of EIS further increasing (curve e). With the increased negative charge from the DNAzymes, the redox current further declined. Subsequently, during linear HCR, the current peak further declined, and the resistance was augmented (curve f). These variations were consistent with the expected increase in electrostatic repulsion between the long double DNA strand and $[Fe(CN)_6]^{-3/-4}$, indicating that the HCR reaction successfully fixed a large number of C-rich sequences.[47] Ultimately, the electrodes were covered with AgNCs, verified by the significantly enlarged semicircle and further reduced redox currents (curve g). Transmission electron microscopy images also showed the synthesis of silver nanoclusters with high yield (Figure S1).

Moreover, to investigate the ECL capability of our sensing platform, ECL measurements were taken with stepwise modified electrodes for some important steps. The ECL signal and corresponding strength analysis indicated that the background ECL signal of the bare GCE and DNA-modified electrodes were extremely low (curves a−c).[36] With the implementation of in situ synthesis of AgNCs, the ECL signal of the electrode without a target miRNA displays no significant change from the background (curve d). In the presence of a target miRNA, the electrode displayed evidently enhanced ECL responses (curve e). The comparative results clearly show that the ECL signal on the electrode changes significantly in the presence of the target with a low background signal, which demonstrates the good performance of our ECL sensor.

ECL Analysis of Myocardial miRNAs and the Myocardial miRNA Group. To assess the quantitative detection capability of our biosensor, it was applied to detect different AMI-related miRNAs in different concentrations (Figure 3). We first chose the commonly used miRNA-499 as the representative to explore the sensitivity and linear range of detection. With the increase in miRNA concentration, ECL intensity increased step by step. By comparing and analyzing the ECL curves, we found that miRNA-499 could induce distinguishable changes in ECL signals, and we concluded that the lowest detectable concentration of miRNA-499 was 0.1 fM (Figure 3A). As shown in Figure 3B, to meet the requirements of practical quantitative detection, the linear relationship between ECL intensity and known logarithmic concentration of miRNA-499 from 0.1 fM to 1 nM was plotted with a limit of detection (LOD) of 52.5 aM (S/N = 3).

To expand the application of the detection platform, two randomly selected myocardial miRNAs (miRNA-328 and miRNA-208) were also tested. According to ECL intensity

https://doi.org/10.1021/acs.analchem.1c01051
Anal. Chem. 2021, 93, 7516−7522

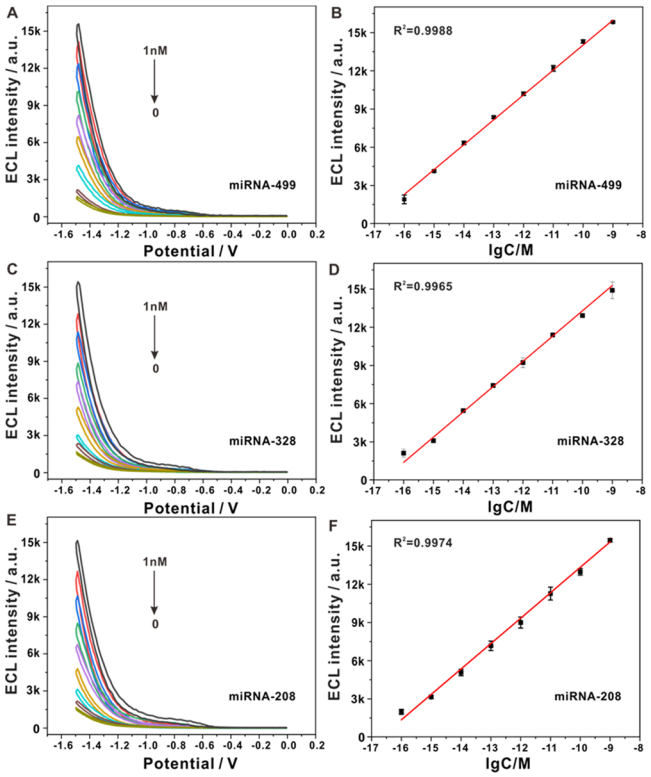

Figure 3. ECL intensity−potential curves with varying concentrations of (A) miRNA-499, (C) miRNA-328, and (E) miRNA-208; corresponding calibration curves by plotting ECL intensity against logarithmic concentrations of (B) miRNA-499, (D) miRNA-328, and (F) miRNA-208.

curves, 0.1 fM of arbitrary miRNA can cause discernible changes (Figure 3D,F). For both miRNA-328 and miRNA-208, a good linear relationship was established between ECL intensity and the logarithm of concentration from 0.1 fM to 1 nM (Figure 3C,E). Meanwhile, the LOD of miRNA-328 was calculated to be 47.9 aM (S/N = 3), and the LOD of miRNA-208 was even lower as 29.6 aM (S/N = 3). To further support the detection results and explain the difference between the LOD, the disassociation constant (K_d) between the target myocardial miRNA and auxiliary strands was calculated according to the method reported previously.[48] The K_d values for miRNA-499, miRNA-328, and miRNA-208 are 66.0, 59.8, and 53.3 nM, respectively (Figure S3). This indicates that these miRNAs have similar affinity with auxiliary strands, and miRNA-208 binds to auxiliary strands with stronger affinity than the other two miRNAs. The calculate K_a values are consistent with the difference in the LOD and further support the detection result. In addition, we compared other biosensors (Table S1) that have been reported for miRNA detection in myocardial infarction. Our results demonstrate that our platform is capable of both a lower detection limit and a wider linear detection range than existing methods. It is also worth noting that our biosensor can easily test multiple samples and can be used in a wide range of applications.

Stability is an important criterion to measure ECL biosensor performance. To investigate the stability of our proposed biosensor, continuous cyclic potential scanning was executed with 100 fM miRNA-499 from −1.6 to 0.0 V. Fifteen ECL intensity curves obtained from continuous cyclic scans showed a high degree of consistency with an RSD of 0.53% (Figure 4A), indicating stability and reliability of the ECL signal. Also, parallel measurements of different targets with an RSD of <5%

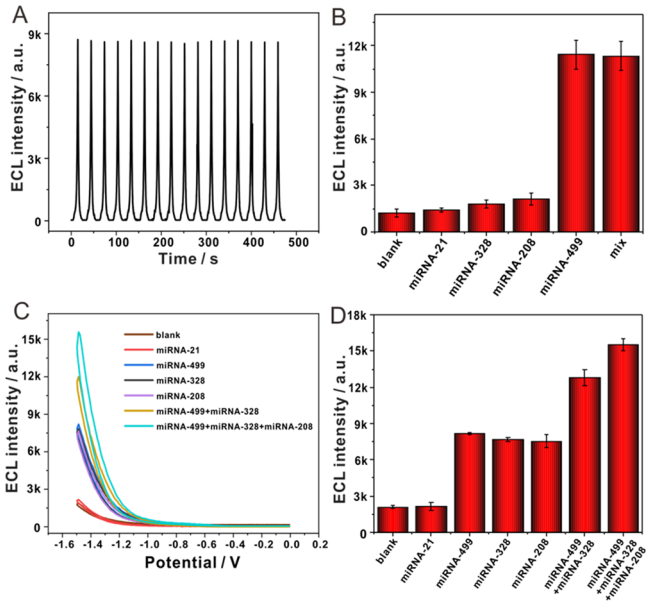

Figure 4. (A) Multiple cycle assays of miRNA-499 with a concentration of 100 fM taken as an example to demonstrate the stability of the biosensor. (B) Specificity of the aptasensor for a single myocardial miRNA tested with different targets. Except for miRNA-499 with a concentration of 10 pM, concentrations used for other miRNAs were 100 pM. (C) ECL intensity−potential curves and (D) ECL intensity to demonstrate the specificity of the proposed biosensor for multiple myocardial miRNAs and myocardial miRNA groups. The concentration of every miRNA in all samples was 1 pM.

revealed the reproducibility of the proposed ECL biosensor (Figure 4B). The specificity of myocardial miRNAs is a challenging task for this biosensor since multiple homologous miRNAs often coexist in blood. To evaluate the specificity of the assay, we tested selectivity for miRNA-499 by replacing it with other coexisting myocardial miRNAs at higher concentrations. The comparative experimental results show that 10 pM miRNA-499 can induce significant ECL response, while the ECL signal corresponding to other miRNAs with higher concentration is almost identical to a blank signal. In addition, for the mixture sample that contains all the above three miRNAs (100 pM) and miRNA-499 (10 pM only), the detected ECL signal appears to be caused by miRNA-499 alone (Figure 4B). The comparative test results successfully demonstrate the high specificity of the biosensor.

Since a variety of miRNAs are often present during the onset of AMI with extremely low levels, extending the detection object to a group composed of multiple related miRNAs or any related miRNA in the group can result in a faster and earlier diagnosis of the disease.[49−51] To better simulate actual conditions, we extended the detection range of our sensor to the group composed of multiple myocardial miRNAs. We performed selective tests on simulated cohorts composed of two myocardial miRNAs and cohorts composed of three myocardial miRNAs (Figure 4C,D). By adding three auxiliary sequences simultaneously, the response to different groups is achieved without affecting the signal of a single target. We are able to elicit a signal response through group detection when the concentration of a single target is low due to the improved

https://doi.org/10.1021/acs.analchem.1c01051
Anal. Chem. 2021, 93, 7516−7522

ECL signal of miRNA groups. Although the response intensity to the group is lower than the sum of three individual signals, detecting myocardial miRNA groups still has great application prospects in clinical analysis.

Application in Serum Samples. To develop our method for clinical use, we analyzed individual miRNA and miRNA groups in 10% serum. As shown in Figure 5, there is no

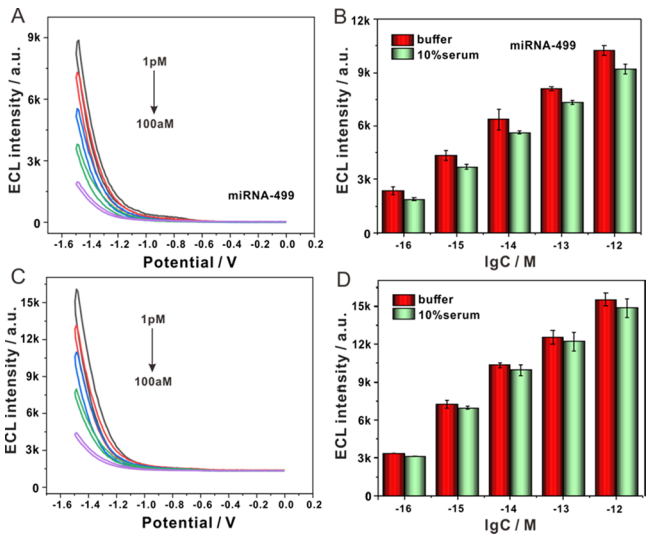

Figure 5. Application in serum samples. (A) ECL intensity−potential curves of miRNA-499 at different concentrations in 10% serum. (B) Comparison of miRNA-499 ECL intensity between TE buffer and 10% serum. (C) ECL intensity−potential curves of the myocardial miRNA group (made up of three miRNAs in equal quantities) in 10% serum. (D) Comparison of the myocardial miRNA group ECL intensity between TE buffer and 10% serum.

significant difference between the analysis results in serum and those in the buffer, indicating good detection performance of our sensing platform in the serum sample. In addition, accurate analysis of the myocardial miRNA group can still be achieved in serum, demonstrating the flexibility of the detection scheme.

CONCLUSIONS

We have demonstrated a multitargeted ECL biosensor for myocardial miRNA detection by combining DNAzyme-assisted targeting of circulating miRNAs and HCR that induced AgNC synthesis in situ. We designed a versatile probe that not only contains part of the DNAzyme component but also contains the HCR trigger sequence. With the help of the versatile probe, multiple miRNAs and myocardial miRNA groups can be recognized only by adjusting the auxiliary sequences; thus, numerous HCR trigger chains can be released to trigger the second amplification, a large number of C-rich sequences are attached to the electrode, and AgNCs can be synthesized in situ on C-rich chains, which give out strong ECL signals. With outstanding flexibility and specificity, our well-designed biosensor can accommodate multiple miRNAs and miRNA groups and has great prospects in the diagnosis of AMI.

ASSOCIATED CONTENT

Supporting Information

The Supporting Information is available free of charge at https://pubs.acs.org/doi/10.1021/acs.analchem.1c01051.

TEM images for AuNPs, TEM images for AgNCs, ECL measurement of the dissociation constant, table for all used gene sequences, and comparison table of biosensors for the detection of AMI-related miRNAs (PDF)

AUTHOR INFORMATION

Corresponding Author

Kui Zhang − *School of Chemistry and Chemical Engineering, Anhui University of Technology, Ma'anshan, Anhui 243032, P. R. China;* orcid.org/0000-0002-5634-9952; Email: zhangkui@mail.ustc.edu.cn

Authors

Yudie Sun − *School of Chemistry and Chemical Engineering, Anhui University of Technology, Ma'anshan, Anhui 243032, P. R. China;* orcid.org/0000-0002-1053-7472

La Fang − *School of Chemistry and Chemical Engineering, Anhui University of Technology, Ma'anshan, Anhui 243032, P. R. China*

Zhe Zhang − *School of Chemistry and Chemical Engineering, Anhui University of Technology, Ma'anshan, Anhui 243032, P. R. China*

Yang Yi − *School of Chemistry and Chemical Engineering, Anhui University of Technology, Ma'anshan, Anhui 243032, P. R. China*

Shengjun Liu − *School of Chemistry and Chemical Engineering, Anhui University of Technology, Ma'anshan, Anhui 243032, P. R. China*

Qian Chen − *School of Chemistry and Chemical Engineering, Anhui University of Technology, Ma'anshan, Anhui 243032, P. R. China*

Jian Zhang − *School of Chemistry and Chemical Engineering, Anhui University of Technology, Ma'anshan, Anhui 243032, P. R. China*

Cheng Zhang − *School of Chemistry and Chemical Engineering, Anhui University of Technology, Ma'anshan, Anhui 243032, P. R. China*

Lifang He − *School of Chemistry and Chemical Engineering, Anhui University of Technology, Ma'anshan, Anhui 243032, P. R. China;* orcid.org/0000-0001-5164-8956

Complete contact information is available at: https://pubs.acs.org/10.1021/acs.analchem.1c01051

Author Contributions

‖Y.S. and L.F. contributed equally to the paper as the first authors.

Notes

The authors declare no competing financial interest.

ACKNOWLEDGMENTS

We thank Dr. Xuezhong Wang in the Ma'anshan First People's Hospital for providing all used serum in this work. This work was supported by the National Natural Science Foundation of China (nos. 22004003 and 21976002) and the Anhui Provincial Natural Science Foundation for Distinguished Young Scholars (2008085J11).

REFERENCES

(1) Kalinich, M.; Haber, D. A. *Science* **2018**, *359*, 866−867.
(2) Leal, A.; van Grieken, N. C. T.; Palsgrove, D. N.; Phallen, J.; Medina, J. E.; Hruban, C.; Broeckaert, M. A. M.; Anagnostou, V.;

Adleff, V.; Bruhm, D. C.; Canzoniero, J. V.; Fiksel, J.; Nordsmark, M.; Warmerdam, F. A. R. M.; Verheul, H. M. W.; van Spronsen, D. J.; Beerepoot, L. V.; Geenen, M. M.; Portielje, J. E. A.; Jansen, E. P. M.; van Sandick, J.; Kranenbarg, E. M.-K.; van Laarhoven, H. W. M.; van der Peet, D. L.; van de Velde, C. J. H.; Verheij, M.; Fijneman, R.; Scharpf, R. B.; Meijer, G. A.; Cats, A.; Velculescu, V. E. *Nat. Commun.* **2020**, *11*, 525.
(3) Boon, R. A.; Dimmeler, S. *Nat. Rev. Cardiol.* **2015**, *12*, 135.
(4) Ma, W.; Fu, P.; Sun, M.; Xu, L.; Kuang, H.; Xu, C. *J. Am. Chem. Soc.* **2017**, *139*, 11752−11759.
(5) Tavallaie, R.; McCarroll, J.; Le Grand, M.; Ariotti, N.; Schuhmann, W.; Bakker, E.; Tilley, R. D.; Hibbert, D. B.; Kavallaris, M.; Gooding, J. J. *Nat. Nanotechnol.* **2018**, *13*, 1066−1071.
(6) Gibbings, D. J.; Ciaudo, C.; Erhardt, M.; Voinnet, O. *Nat. Cell Biol.* **2009**, *11*, 1143−1149.
(7) D'alessandra, Y.; Devanna, P.; Limana, F.; Straino, S.; Di Carlo, A.; Brambilla, P. G.; Rubino, M.; Carena, M. C.; Spazzafumo, L.; De Simone, M.; Micheli, B.; Biglioli, P.; Achilli, F.; Martelli, F.; Maggiolini, S.; Marenzi, G.; Pompilio, G.; Capogrossi, M. C. *Eur. Heart J.* **2010**, *31*, 2765−2773.
(8) Ludwig, N.; Leidinger, P.; Becker, K.; Backes, C.; Fehlmann, T.; Pallasch, C.; Rheinheimer, S.; Meder, B.; Stähler, C.; Meese, E.; Keller, A. *Nucleic Acids Res.* **2016**, *44*, 3865−3877.
(9) Deng, R.; Zhang, K.; Li, J. *Acc. Chem. Res.* **2017**, *50*, 1059−1068.
(10) Yang, H.; Qin, X.; Wang, H.; Zhao, X.; Liu, Y.; Wo, H.-T.; Liu, C.; Nishiga, M.; Chen, H.; Ge, J.; Sayed, N.; Abilez, O. J.; Ding, D.; Heilshorn, S. C.; Li, K. *ACS Nano* **2019**, *13*, 9880−9894.
(11) Bejerano, T.; Etzion, S.; Elyagon, S.; Etzion, Y.; Cohen, S. *Nano Lett.* **2018**, *18*, 5885−5891.
(12) Sun, T.; Dong, Y.-H.; Du, W.; Shi, C.-Y.; Wang, K.; Tariq, M.-A.; Wang, J.-X.; Li, P.-F. *Int. J. Mol. Sci.* **2017**, *18*, 745.
(13) Zhu, L.; Zhang, M.; Ye, J.; Yan, M.; Zhu, Q.; Huang, J.; Yang, X. *Anal. Chem.* **2020**, *92*, 8614−8622.
(14) Wexler, Y.; Nussinovitch, U. *Cell* **2020**, 9.
(15) Wang, C.; Jing, Q. *Acta Pharmacol. Sin.* **2018**, *39*, 1110−1119.
(16) Qiu, Z.; Shu, J.; Liu, J.; Tang, D. *Anal. Chem.* **2018**, *91*, 1260−1268.
(17) Mi, L.; Sun, Y.; Shi, L.; Li, T. *ACS Appl. Mater. Interfaces* **2020**, *12*, 7879−7887.
(18) Shi, L.; Sun, Y.; Mi, L.; Li, T. *ACS Sens.* **2019**, *4*, 3219−3226.
(19) Sun, Y.; Shi, L.; Wang, Q.; Mi, L.; Li, T. *Anal. Chem.* **2019**, *91*, 3652−3658.
(20) Sun, Y.; Li, T. *Anal. Chem.* **2018**, *90*, 11614−11621.
(21) Sun, Y.; Wang, Q.; Mi, L.; Shi, L.; Li, T. *Anal. Chem.* **2019**, *91*, 12948−12953.
(22) Ye, J.; Liu, G.; Yan, M.; Zhu, Q.; Zhu, L.; Huang, J.; Yang, X. *Anal. Chem.* **2019**, *91*, 13237−13243.
(23) Wang, J.; Haghighatbin, M. A.; Shen, W.; Mi, L.; Cui, H. *Anal. Chem.* **2020**, *92*, 7062−7070.
(24) Zhu, L.; Ye, J.; Wang, S.; Yan, M.; Zhu, Q.; Huang, J.; Yang, X. *Chem. Commun.* **2019**, *55*, 11551−11554.
(25) Chen, J.; Pan, J.; Chen, S. *Chem. Sci.* **2018**, *9*, 300−306.
(26) Zhang, Z.; Balogh, D.; Wang, F.; Willner, I. *J. Am. Chem. Soc.* **2013**, *135*, 1934−1940.
(27) Hu, L.; Lu, C. H.; Willner, I. *Nano Lett.* **2015**, *15*, 2099−2103.
(28) Freage, L.; Wang, F.; Orbach, R.; Willner, I. *Anal. Chem.* **2014**, *86*, 11326−11333.
(29) Kou, B.; Chai, Y.; Yuan, Y.; Yuan, R. *Anal. Chem.* **2018**, *90*, 10701−10706.
(30) Yang, L.; Wu, Q.; Chen, Y.; Liu, X.; Wang, F.; Zhou, X. *ACS Sens.* **2019**, *4*, 110−117.
(31) Wan, S.; Zhang, L.; Wang, S.; Liu, Y.; Wu, C.; Cui, C.; Sun, H.; Shi, M.; Jiang, Y.; Li, L.; Qiu, L.; Tan, W. *J. Am. Chem. Soc.* **2017**, *139*, 5289−5292.
(32) Jörg, P.; Ahner, T. T.; Delissen, F.; Sokolov, S.; Emmerling, F.; Thünemann, A. F.; Kraehnert, R. *J. Am. Chem. Soc.* **2010**, *132*, 1296−1301.
(33) Ge, J.; Zhao, Y.; Li, C.; Jie, G. *Anal. Chem.* **2019**, *91*, 3546−3554.
(34) Chen, Y. X.; Huang, K. J.; Niu, K. X. *Biosens. Bioelectron.* **2018**, *99*, 612−624.
(35) Yang, C.; Shi, K.; Dou, B.; Xiang, Y.; Chai, Y.; Yuan, R. *ACS Appl. Mater. Interfaces* **2015**, *7*, 1188−1193.
(36) Feng, X.; Han, T.; Xiong, Y.; Wang, S.; Dai, T.; Chen, J.; Zhang, X.; Wang, G. *ACS Sens.* **2019**, *4*, 1633−1640.
(37) Lu, S.; Wang, S.; Zhao, J.; Sun, J.; Yang, X. *Anal. Chem.* **2017**, *89*, 8429−8436.
(38) Liu, L.; Liu, J. W.; Huang, Z. M.; Wu, H.; Li, N.; Tang, L. J.; Jiang, J. H. *Anal. Chem.* **2017**, *89*, 6944−6947.
(39) Liu, H.; Li, Q.; Li, M.; Ma, S.; Liu, D. *Anal. Chem.* **2017**, *89*, 4776−4780.
(40) Zhou, H.; Liu, J.; Xu, J. J.; Zhang, S. S.; Chen, H. Y. *Chem. Soc. Rev.* **2018**, *47*, 1996−2019.
(41) Nie, Y.; Zhang, P.; Wang, H.; Zhuo, Y.; Chai, Y.; Yuan, R. *Anal. Chem.* **2017**, *89*, 12821−12827.
(42) Wang, H.; Yuan, Y.; Zhuo, Y.; Chai, Y.; Yuan, R. *Anal. Chem.* **2016**, *88*, 2258−2265.
(43) Cui, A.; Zhang, J.; Bai, W.; Sun, H.; Bao, L.; Ma, F.; Li, Y. *Biosens. Bioelectron.* **2019**, *144*, 111664.
(44) Zhang, X.; Li, W.; Zhou, Y.; Chai, Y.; Yuan, R. *Biosens. Bioelectron.* **2019**, *135*, 8−13.
(45) Zheng, Y. N.; Liang, W. B.; Xiong, C. Y.; Zhuo, Y.; Chai, Y. Q.; Yuan, R. *Anal. Chem.* **2017**, *89*, 9445−9451.
(46) Lu, L.; Yang, B.; Kang, T. *Appl. Surf. Sci.* **2017**, *426*, 597−604.
(47) Li, C.; Lu, W.; Zhou, X.; Pang, M.; Luo, X. *Anal. Chem.* **2018**, *90*, 14239−14246.
(48) Li, S.; Chen, D.; Zhou, Q.; Wang, W.; Gao, L.; Jiang, J.; Liang, H.; Liu, Y.; Liang, G.; Cui, H. *Anal. Chem.* **2014**, *86*, 5559−5566.
(49) Singh, R. P.; Massachi, I.; Manickavel, S.; Singh, S.; Rao, N. P.; Hasan, S.; Mc Curdy, D. K.; Sharma, S.; Wong, D.; Hahn, B. H.; Rehimi, H. *Autoimmun. Rev.* **2013**, *12*, 1160−1165.
(50) Fan, P.-C.; Chen, C.-C.; Peng, C.-C.; Chang, C.-H.; Yang, C.-H.; Yang, C.; Chu, L. J.; Chen, Y.-C.; Yang, C.-W.; Chang, Y.-S.; Chu, P.-H. *J. Transl. Med.* **2019**, *17*, 1−12.
(51) Polyakova, E. A.; Zaraiskii, M. I.; Mikhaylov, E. N.; Baranova, E. I.; Galagudza, M. M.; Shlyakhto, E. V. *Int. J. Cardiol.* **2021**, *322*, 9−15.

https://doi.org/10.1021/acs.analchem.1c01051
Anal. Chem. 2021, 93, 7516−7522